Effect of Gamma Rays on Zn/Cu Doped Strontium Borate Glass System for Dosimetric Applications

Eman Mohammed
National Center for Radiation Research and Technology (NCRRT)
Sameh Gafar (gafarsameh@yahoo.com)
National Center for Radiation Research and Technology (NCRRT)

Research Article

Keywords: alkali metal, glass, ions, γ-rays, and dosimeters

Posted Date: October 15th, 2021

DOI: https://doi.org/10.21203/rs.3.rs-968075/v1

Abstract

Two alkali metal strontium borate glass systems containing Cu^{2+} or Zn^{2+} ions (0.15 mol. %) have been prepared by the conventional melt annealing method, then some of their dosimetric measurements have been performed. The two glass systems were checked by ultraviolet-visible light measurement, where Cu^{2+} ions reveal a sharp peak in the UV region at 320 nm as Cu^{+} and a broad visible band at ~ 735 nm as Cu^{2+}. However, Zn^{2+} ions reveal two sharp peaks at 290 & 300 nm related to its divalent state (Zn^{2+}). Upon γ-rays, glass is sensitive to the absorbed dose in the range 0.4 to 15 kGy, revealing its light absorption. A gradual decrease in optical absorbance intensity and DC electrical conductivity was detected with the progressive irradiation. While, a gradual increase in optical energy band gap (Eopt) and electron paramagnetic resonance (EPR) was observed. The presence of transition metal ions (TM) with a variable configuration helps to trap the radiolytic electrons or holes during the color center recovery rates. All the dosimetry characteristics of EPR spectrum, UV-Vis spectrophotometer has high color stability and excellent short-term and long-term stability of the studied glass dosimeters, revealing its applications in medical sterilization and food irradiation processing.

Highlights

- Preparation of two glass systems containing Cu^{2+} or Zn^{2+} ions.
- The conventional melt annealing method, then some of their dosimetric measurements have been performed.
- The two glass systems were checked by ultraviolet-visible light measurement and EPR, and TM.
- Upon gamma irradiation undergoes radiation inducing an optical change in the absorption of the spectrum and EPR spectroscopy of the prepared glass.
- The absorbed dose for these dosimeters was found to be from 0.4 to 15 kGy.
- These dosimeters can be applied in many fields in food irradiation processing, irradiation applications, medical sterilization.

Introduction

Due to the recent extensive use of ionizing radiations in many medical, industrial and agricultural applications [1-3], researchers are encouraged to study new host materials with suitable features for dosimetric applications [1-4]. Moreover, there are many types and shapes of dosimeters; thin plastic polymeric films [1-4], solution dosimeters [5-9], very sensitive gel dosimeters [6-10], and EPR dosimeters [11,12]. These types are based on their sensitivity to gamma-ray sort reveal that gel dosimeters or EPR dosimeters are more sensitive than liquid or film dosimeters [10,11,12]. Borate glasses are very interesting candidates to be used as a glass former in radiation dosimetry applications. Because they have many specific advantages for this target for example; (a) their effective atomic number is very close to human tissues (Zeff = 7.42), which is the most insignificant feature of personal dosimeter [13, 14-16], (b) high sensitivity to external radiation doses, (c) good chemical structure and mechanical strength (d)

ease of preparation, shaping and low cost (e) wide electronic band gap and stability, and (f) good host for modifying ions like rare earth and transition metal ions [13, 16,17]. B_2O_3 has two forms of boron coordination; three coordinated triangle BO_3 units and the four coordinated $[BO_4]$– groups. BO_3 groups are only present in the pure B_2O_3 glass according to Nattapol et al. [18]. However, under the influence of some factors like the incorporation of modifier ions or irradiation process, some of the triangle BO_3 units are converted into tetrahedral BO_4^- groups by generating more non-bridging oxygens NBOs.

For improving the performance of borate glasses and increasing their specific characteristics like durability and stability, alkaline earth oxides have been incorporated in borate glass structure. For example, Na^+ ions tend to increase the glass stability, moisture absorption and acts as a flux to decrease the melting temperature required for preparing the glass. SrO improves the chemical resistance of the glass by stabilizing the glass structure [19, 20] and provides the possible usage of glass in many optical and biomedical applications [20]. Introducing transition metal ions into a borate glass structure like $Cu^{2+}$and Zn^{2+} ions improve the strength of the glass, enhances their electron emission and creates a deep stable complex defect [13,14]. Transition metal ions have a special character to acquire the glass its precise properties, e.g. low annealing temperature, good electrical conductivity and, reasonable infrared transmission properties [21]. This performance of TM ions is due to their capability to modify their valence coordination states, since the outer electron orbitals are highly sensitive to any surrounding electronic changes specially the $3d^1$ transition metal ions e.g. Cu^{2+} and Zn^{2+} ions [22, 23].

The amorphous structure of the glass comprises mostly of pre-existing intrinsic defects e.g. oxygen vacancies, NBO, or flaws created by the high energetic electrons. Exposing glass to gamma radiation causes some atomic displacements in the glass structure and changes NBO number and/or breaking bonds. This influence is controlled by the glass composition, its intrinsic defects and the dose of irradiation [21]. Ionizing radiation causes the production of electron–hole pairs which usually absorb visible light (color centers) so, it affects the glass optical properties and then its radiation sensitivity and efficiency [24]. Many instrumental techniques can be used to identify the formed induced defects in the glass like optical and ESR measurements.

This research study targets to investigate two types of alkali strontium borate glass systems with the composition of; 60-x B_2O_3 + 25 SrO + 15 Na_2O + x where x=0.15 mol% CuO/ZnO, and study some of their dosimetric properties against gamma radiation dose range (0.5-15 kGy) such as, UV-visible absorbance, optical energy band gap Eopt, DC electrical conductivity (EC), Electron paramagnetic resonance (EPR), color stability, response curve functions, short and long term stability. Then from the results analysis, we can determine the most useful dose range of the two glass dosimeters as well as their specific dosimetric properties used in many fields in food-irradiation processing, and medical sterilization and many industrial applications.

Materials And Methods

Using the traditional melting annealing method, two glass systems of strontium borate have been prepared with the composition of (60-x) B_2O_3+ 25 SrO +15 Na_2O +x where x= 0.15 CuO or 0.15 ZnO. The following bought chemical materials (Sigma Aldrich Company with purity 99.9%) were used in the preparation of the glasses; H_3BO_3, $SrCO_3$, Na_2CO_3, and CuO/ ZnO. Accurately weighed batches were melted in a muffle furnace at 950 ◦C for ~ 90 min with a careful stirring at each 30 min time intervals to realize the homogeneity of the glass melt. The homogenized melts were then poured into preheated stainless steel molds to transfer directly to an annealing muffle controlled at 300 ◦C for removing stress and/or thermal strain residues in the glasses. After 1 hr the annealing muffle was switched off to leave the prepared glass samples to cool to the RT with a rate of 30 ◦C/h. Polished equal thickness (2 mm ± 0.1 mm) or fine powder samples were organized for the required measuring techniques.

The optical absorbance spectra were measured by a double-beam UV-visible spectrophotometer (Jasco, V-570 UV-VIS-NIR Rel-100 Japan). Programmable height resistance electrometer (KEITHLY 6517B) with a reliable, fast response together with the power supply was used to measure the electrical conductivity of the glass samples by detecting resistivity at constant current and voltage. Where the specific electrical conductivity (σ) can be attained from the relation; σ = LA x 1/r where L; the thickness of the glass sample in cm, A, the cross section area in cm^2 and r, the measured resistance in ohm.

EPR measurements were carried out using a Bruker EMX spectrometer (X-Gand, Germany); where the cavity used the standard Bruker ER 4102 rectangular levity. The operating conditions for EPR spectrometers were as follows: microwave power 2 mW. Modulation amplitude 3 Gauss, sweep width = 200 G, microwave frequency = 9.72 GHz, time constant = 81.92 ms and sweep time 20.48 s. Stability of the EPR spectrometers sensitive was checked before and after each series of measurements using reference alanine dosimeters irradiated to know the dose. The intensity of the ESR spectra was measured as the peak– to– peak high of the broad EPR single divided by the peak–to peak light of reference signal from a strong pitch sample, divided by the density of the glass samples in the tube (g/length) as a function of irradiation dose in kGy. All EPR measurements were carried out at room temperature 25±2^o, Co-60 gamma cell with a dose rate = 0.971 kGy/h at 25 ± 5 °C was utilized as a gamma ray source for irradiation processes.

Results And Discussion

3.1 Optical UV- visible measurements

3.1.1 Optical UV- visible spectra before and after gamma irradiation

Changes in the glass lattice because of doping an element or irradiation can be determined by optical UV spectroscopy, where it gives information about radiation-induced defect centers [25].

The existence of TM ions even in very small concentrations reasons an electron transfer effect, including the movement of an electron from a coordinating oxygen atom orbital to the metal ion orbital. Consequently an obvious UV band is determined on the UV spectrum of TM ions containing glasses [21].

Fig.1 illustrates the UV- visible optical spectra of Cu and Zn borate glasses. It is observed from the figure that there are small UV peaks appeared in both glasses in the UV region 200–270 nm, correlated to the presence of the triplet Fe^{3+} impurities accompanied to the chemical materials used in the glass preparation process [16, 17, 23]. For Cu- glass there are two observed peaks are detected; (a) sharp peak in the UV region at 320 nm (b) a broad visible-near IR band at ~ 735 nm. CuO can exist in two valence states; the monovalent Cu^{1+} ($3d^{10}$) and the divalent state Cu^{2+} ($3d^{9}$). Therefore, it participates in the glass network either in the form of CuO^{4} or CuO^{6}, respectively [26]. Cu^{1+} has five occupied d-orbitals therefore; it does not produce separate coloring, however, the cupric Cu^{2+} gives definite coloring centers in the visible region because of the creation of strong Cu^{2+} tetragonal distortion in octahedral units [27]. Therefore, Cu-containing glass displays a bluish green color demonstrating the presence of Cu^{2+} divalent state referring to the broad visible-near IR peak at ~ 735 nm. But, the identification of the monovalent Cu^{+} ions seems to be restricted to the observed UV sharp peak at 320 nm [28]. For Zn- glass, there are two detected distinct sharp peaks in the UV region at ~ 290 and 300 nm without the appearance of the peaks in the visible region. This behavior refers to the presence of Zn ions of their divalent state as Zn^{2+} ($3d^{10}$) and explaining in turn the white colorless of Zn- glass.

Fig.2 (a & b) illustrates the effect of progressive γ-irradiation on the optical behavior of the studied Cu and Zn glasses; respectively. From the figures it is observed that there is a gradual decrease in the absorbance intensity for the both glasses with increasing the absorbed doses. This performance can be discussed according to the direct effect of gamma radiation on the studied glasses which directly affects the host glass matrix by changing the number of bridging oxygens BO and non-bridging oxygens NBO via creating or breaking bonds with the neighboring oxygens and atoms. This effect of such ionizing radiation takes place through some photochemical reactions either photo-oxidation or photo-reduction processes of TM ions in the lower valence states. For example the photo-oxidation process of cuprous Cu^{1+}, the lower valence state of Cu into cupric Cu^{2+}, the higher oxidation of Cu [23, 29,30].

$$Cu^{1+} + h\upsilon \leftrightarrow Cu^{2+} + e^{-} + h^{+} \qquad (1)$$

This recommendation was approved by [31], who assumed that metal ions (such as Ce^{3+}, U^{4+}) as well as d^{10} s^{2} ions have the capability to absorb radiation via some electronic transitions including energetic changes when an electron transfer takes place from an atomic orbital to another [28].

According to the observed spectra in Fig.2, the gradual decrease in the UV absorbance intensity may be related to the formation of more bridging oxygens with the progressive irradiation of glasses. Because of the ability of transition metal ions to contract with the intrinsic defects in the glassy network by capturing or trapping the radiolytic electrons or holes and then the formation of intrinsic color centers recovery rates, they are so called as “potential traps” [32]. Trapping or capturing processes depends essentially on the doped TM ion; its kind and concentration, in addition to the main composition of the host glass matrix [33]. Since the main composition of the studied glasses (60-x B_2O_3+ 25 SrO+ 15 Na_2O) and the

concentration of TM (x=15 mol.) are constant, then the optical behavior depends only on the type of the transition metal ion Cu or Zn as well as the dose of radiation.

3.1.2 Optical response curve

The optical density readout was done at two wavelengths 320 and 300 for Cu and Zn glass samples, respectively. Fig. 3 shows the response curves of Cu and Zn borate glass samples in terms of change in absorption coefficient, ΔA. mm^{-1} at 320 and 300 nm, versus the absorbed dose, in line with the relation ($\Delta A = A_o - A_i$), wherein A_o and A_i are the values of the absorption coefficient for the un-irradiated and irradiated glasses; respectively. From the response curve, the effective dose range of the two glass systems is between 0.4 and 15 kGy depending upon the glass structure and the sort of the introduced transition metal ion. Response curves show additionally that both Cu and Zn glass samples are sensitive to gamma-rays in the dose range between 0.4 and 15 kGy and then their possible use as radiation dosimeters.

3.1.3 Post irradiation stability of Cu/ Zn glass samples

Both Cu and Zn borate glass system irradiated with 3 kGy, have been stored at room temperature (25^{o}C ±2) in the dark and under laboratory fluorescent light. The absorbance of the two glass samples was measured at 320 and 300 nm exclusive time intervals through the post-irradiation storage duration of two months. Change in absorbance at the two wavelengths at one of a kind conditions of storage as a characteristic of storage time is relative to that when storage as indicated in Fig.4. From this figure, it's far found that the two irradiated glasses exhibit good stability beneath the storage conditions except for the primary 7 days.

3.1.4 Optical energy band gap Eopt

Optical energy band gap (Eopt) can be identified by by plotting $(\alpha h\nu)^n$ against the incident photon energy (hv) as given in Eq (2) [34];

$$\alpha h\nu = [\alpha o(h\nu - E_{opt})^n]/h\nu \quad (2)$$

Where α (v) is the absorption coefficient, αo is a constant, n is a constant depends on the mechanism of electron transition; direct or indirect, allowed or forbidden [21]. In the amorphous structure of the glass system; n can be taken as 0.5 for the indirect allowed transitions.

The optical energy band gap is linked directly to the cross-linking between individual atoms in the glass structure. Therefore, it is controlled essentially by the glass composition and any structural modifications take place because of specific factors like the addition of modifier ions and/or irradiation processes. Eopt can be adjusted by generating positively or negatively charged defect centers "color center" causing the formation of energy levels between the original bands [24]. Fig.5 (a &b) show the linear plots of Eopt values for the studied Cu and Zn borate glasses before and after the progressive irradiation in the dose

range 0.4 - 15 kGy, where there is a gradual increase in the Eopt values with increasing the dose of radiation. This behavior can be correlated directly to the effect of radiation in making some structural changes inside the glass matrix by changing the oxygen bond strength of the glassy network [27]. Mott and Davis [34] have assumed that the alteration in Eopt of the glass is related to the conversion between bridging oxygens and non-bridging oxygens. According to the response curve shown in Fig.6, the gradual increase in Eopt with irradiation doses may be due to the combination between positive holes and negative electrons and then the conversion of some NBOs into BO, creating new bonds with lower defect centers and more closed structure. This process introduces a large energy gap between the ground and excited levels of atoms giving in turn larger Eopt. Some authors [35, 36] have reported that rising in the bridging oxygens number gives more covalent bonds and reinforces the bond strengths in the glass structure causing a large splitting between the valence and conduction bands or higher Eopt values. The presence of 3d transition metal ions in the glass structure like Cu^{2+} or Zn^{2+} ions provides this process because of their variable configuration [23] and their tendency to change the outer electronic configurations. The progressive increase of Eopt with irradiation refers also to the sensitivity of Eopt values of the studied glasses to the dose of radiation.

3. 2 Electron paramagnetic resonance measurements

3.2.1 EPR spectra of free radical development of the glass samples

EPR is a very interesting and perfect measuring instrument for testing dosimetric systems [1-3]. To obtain a reproducible and useful applied dosimeter, it is necessary to obtain main essential requirements such as; the stability of free radicals released by the effect of gamma rays, regular or reproducible changes in the increase of free radicals according to each absorbed dose, as well as the instrumental analysis used in the EPR technique [11,12]. Therefore, the intensity of EPR spectra has been recorded at different time intervals. Fig. 7 demonstrates the measured signal intensities of irradiated and un-irradiated Zn-glass samples where there is a good peak height or signals with a single EPR line. Also, it is observed that the EPR signals begin to develop upon irradiation and its amplitude increases gradually with increasing the absorbed doses of gamma-rays without any change in its shape. So, it can be recorded that Cu and Zn glass samples are sensitive to γ-rays from 0.5 to 12 kGy and from 0.5 to 10 kGy respectively with similar behavior.

Moreover, the EPR signal intensities have been plotted against the square root of the microwave power (range 0-5 mW) as shown in Fig. 8. The power 2.012 mW, corresponding to $P^{1/2}$ = 1.4184 mW has been selected for carrying out the measurements, as it is almost at the upper end of the linear range of the dependence. Furthermore, the intensity of the signals increases in proportion to the square root of microwave power ($P^{1/2}$) up to high microwave power. Consequently, an appropriate set of microwave power level is important for the EPR measurement and dosimeter sensitivity.

3.2.2 EPR Dose-response function

Fig. 9 depicts the dose-response functions of EPR signal intensities for the two types of glass samples in the dose range of 0.5 to 12 and from 0.5 to 10 kGy for Cu/ Zn samples; respectively. Certainly, the signal intensities increase linearly with the increase of absorbed dose (correlation coefficient, r^2= 0.9967049836 in case of Zn, and r^2= 0. 9996760285 in case of Cu glass samples), better linearity and higher r^2 value reflect the validity of the two glass samples to be precise dosimeters for dose process control and the good reproducibility of EPR signal measurements. Based on these consequences those glass samples may be carried out food irradiation processing, medical sterilization, and healthcare sterilization. So that it can be used and applied as radiation dosimeters within the range between 0.5 and 12 kGy relies on the conduct of the form of the introduced transition metal ions.

3.2.3 Stability of glass sample's response

(a) Pre-irradiation Stability

One of the most important dosimetric characteristics of Fig. 10 a and b is the pre-irradiation stability over 63 days of glass samples (Cu/Zn), which was studied by measuring the EPR signals of different types of glass samples during storage periods. The samples are conditioned in the dark and under laboratory fluorescent lights at 33% relative humidity and at room temperature (25 ±2^0 C). From the results, under different storage conditions, no detectable EPR signal was generated during the storage period.

(b) Short term post-irradiation stability

By continuously reporting the EPR spectrum every 10 minutes for 100 minutes, the stability of the radiation-induced paramagnetic center in a 3 kGy glass sample over time is estimated. As shown in Figure 11 (a), the relative response attenuation of the two glass samples during this period was very good.

(c) Long term post-irradiation stability.

The post-irradiation stability of of Cu/ Zn glass samples stored under light and dark irradiation at 33% relative humidity (RH) and at room temperature (25 ± 2 ^{0}C) was investigated. Three small pellet samples were irradiated with a dose of 3 kGy. Measure the signal height of the EPR signal of the studied glass samples immediately after irradiation. The samples were then stocked for approximately 8 weeks, and EPR measurements were taken at various times before this storage period. The post-irradiation stability curve of the glasses is illustrated in Fig. 11 (b). The Long-term stability after irradiation is also excellent, In the first five days of storage after irradiation, the EPR signal only dropped by about 1%. The amount of radical decay comes from the structure of the glass network. The spin–spin interaction belongs to the concentration of spins in the glass samples, which increasing with increasing the spin density in the sample [37, 12].

3.3 Electrical conductivity measurements

Specific electrical conductivity (σ) of the glass samples can be calculated according to the relation σ = (L/A) (1/r), where (σ) is the electrical conductivity of the glass sample, (A) the cross sectional area in cm^2, (L) thickness in cm and (r) the measured resistance in ohm. Fig.12 shows the relation between electrical conductivity of Cu and Zn glasses against the dose of gamma radiation at room temperature. Where, Cu-glass has a relatively higher electrical conductivity (σ) than Zn-glass and an obvious gradual decrease in σ for both glasses with the progressive irradiation is noticed.

Electrical conductivity in glasses depends mainly on the movement of alkali modifier ions that present in the interstitial positions inside the glass network. The most common conducting species in alkali oxide glasses are Na^+ and Li^+ ions since these cations are quite mobile to escape from their positions to the nearby vacancies or interstices in the glass matrix, they are so called as “current carrier ions” [27]. Hence, electrical conductivity of glass is directly proportional to valence and the size of the charge carriers, their concentrations and the ability to move or dispersion under the effect of an external electric field. When the glass contains both alkali ions and transition metal ions, the glass would have a mixed electronic–ionic, pure ionic or pure electronic conduction mechanism [21] according to the internal structure of the glass, concentration of the alkali ions and the electron hopping between the valence states in the TM ion. In the studied glasses, the alkali Sr^{2+} and Na^+ ions act as network, modifying ions creating NBO and enhance the process of charge transport. On the other side, TM ions with their variable configuration can lose or accept electrons to provide the electrical conducting motion by the hopping mechanism of small polarons [38]. The hopping mechanism depends on the type and concentration of TM ion. Cu-glass reveals slightly higher EC than Zn –glass, where Cu^{2+} ions participate as CuO_4 or CuO_6 in the glassy network [26, 27] so, the conduction process is enhanced by the electronic hopping between Cu^{1+} and Cu^{2+} states giving the chance of an easier mobility for the charge carriers. The observed decrease in EC values with irradiation is correlated directly to Eopt values, where increasing Eopt values with radiation dose refers to more BO and more covalent bonds giving closer or more compacted glassy structure. Consequently, a diminish in the mobility of light charge carriers takes place, giving then a relative decrease in electrical conductivity with the progressive irradiation. This behavior shows a good and suitable electric sensitivity of the glasses to gamma radiation doses. Fig.13 shows the long electric stability of the prepared glasses at the room temperature for 40 days. Where the electrical conductivity values of the two glasses give an excellent stability with time of storage.

Conclusion

The following conclusions can be obtained from the data provided in this study:

1-New strontium borate glass systems based on Cu and Zn ions (0.15 mol%) have been prepared and characterized before and after progressive gamma irradiation in the dose range 0.4 -15 kGy.

2-The optical UV- visible spectra shows that the absorption intensity of the two glasses gradually decreases with the increase of radiation dose.

3- Eopt values display a gradual increase with irradiation doses due to the conversion of some NBOs into BO under the effect of irradiation, giving more closed structure with larger Eopt.

4-DC electrical conductivity values of the glasses show a gradual decrease with irradiation, related inversely to Eopt values, since in the more closed glass structure, the chance for moving electric charge carriers is restricted.

5-While, the optical and electrical properties of Cu and Zn strontium borate glasses are highly sensitive to the progressive irradiation, they also reveal good and similar long stability behaviors.

6-The dosimetric characteristics of the glass samples were studied giving significant EPR signal intensity without noise. Upon irradiation, the intensity of the signal increases with the increase in irradiation dose.

7-The useful dose range of these glass samples was found to be from 1 to 12 kGy and 1 to 10 kGy for Cu and Zn glasses, respectively.

8- The response of the two glass dosimeters shows excellent post-irradiation stability (short and long-term stability, EPR studies) where the response decreases only about 1% on the first five days storage periods.

9- Both of pre and post irradiation stability of the two glasses according to color UV-Vis spectrophotometer is in very good manner at different storage conditions.

10- The presence of TM ions with their variable configuration enhance the dosimetric properties of the glasses by changing their valence states through losing or accepting electrons during the irradiation process and changing NBO_S number.

11-The properties of the prepared Cu and Zn strontium borate glass systems suggest their useful application for moderate dose dosimetry applications, e.g. food irradiation processing, medical and industrial applications.

Declarations

Availability of Data and Materials

The datasets used and analyzed during the current study are available from the corresponding author on reasonable request.

Funding

This research did not receive any specific grant from funding agencies in the public, commercial, or not-for-profit sectors.

Conflict-of-Interest Statement

All authors have stated that there is no conflict of interest.

Acknowledgments

This work was financially supported by the National Center for Radiation Research and Technology (NCRRT), the Egyptian Atomic Energy Authority (EAEA), Nasr City, Cairo, Egypt for basic research in the field of radiation technology applications.

References

1. S.M. Gafar, M.A. El-Ahdal, Dosimetric characteristics of 2,6 di-nitro phenol for high dose Dosimetry. Dyes and Pigm **109**, 67–71 (2014)
2. M.A. El-Kelany, S.M. Gafar, M.A. El-Ahdal, Development of ion exchange membrane for possible use in radiation processing dosimetry. Radioanalyt and Nucl Chem **303**(3), 2345–2351 (2014)
3. S.M. Gafar, M.A. Ahdal, A new developed radiochromic film for high-dose dosimetry applications. Dyes and Pigm **114**, 273–277 (2015)
4. S.M. Gafar, M.A. El-Kelany, M.A. El-Ahdal, Low-dose film dosimeter based on mixture of AY and TBPE dyed poly(vinyl alcohol). Dyes and Pigm **140**, 1–5 (2017)
5. W.B. Beshir, S. Eid, S.M. Gafar, S. Ebraheem, Application of solutions of Rhodamine B in dosimetry, Appli radiat isot, 89 (2014), 13–17
6. M.A. El-Kelany, S.M. Gafar, Development of Two Dosimeters for Industrial Use with Low Doses. Nucl Tech &Radiat Prot **32**, 148–154 (2017)
7. S.M. Gafar, N.M. bd El-Kader, Radiation induced degradation of murexide dye in two media for possible use in dosimetric applications. Pigm & Resin Techn **48**(6), 540–546 (2019)
8. S.M. Gafar, N.M. Abd El-Kader, Dosimetric characteristics and applications of cross-linking and degradation of a natural biopolymer Gum Acacia. Radioch Acta **108**(3), 223–229 (2020)
9. S.M. Gafar, N.M. Abd El-Kader, T.M. Mohamed, Radiation-induced Bismuth nanoparticles and its possible use as radiation dosimeter, Radiation Effects and Defects in Solids, 175 (5-6) (2020), 529–539
10. S.M. Gafar, M.A. El-Ahdal, Radiochromic Fuchsine Gel and Its Possible Use for Low Dosimetry Applications. Advanc in Polym Techn **35**(2), 146–151 (2016)
11. S.M. Gafar, M.A. El-Kelany, Radiation induced free-radicals for EPR dosimetry applications. Silic **10**(6), 2671–2675 (2016)
12. S.M. Gafar, Radiation induced free radicals from different milk powders and its possible use as radiation dosimeters milk powder, Radiochemica acta 108 (4)(2020), 321–325
13. S.S. Rojas, K. Yukimitu b, A.S.S. de Camargo c, L.A.O. Nunes c, A.C. Hernandes, Undoped and calcium doped borate glass system for thermoluminescent dosimeter, J. Non-Cryst. Solids 352 (2006), 3608–

3612

14. A. Saidu, H. Wagiran, M.A. Saeed, Y. S. M. Alaje, Thermoluminescence characteristics of zinc lithium borate glass activated with Cu+ ($ZnO–Li_2O–B_2O_3$: Cu+) for radiation dosimetry. J Radioanal Nucl Chem **304**, 627–632 (2015)
15. M.H.A. Mhareb, S. Hashim, S.K. Ghoshal, Y.S.M. Alajerami, M.A. Saleh, N.A.B. Razaka, S.A.B. Azizana, Thermoluminescence properties of lithium magnesium borate glasses system doped with dysprosium oxide. Luminescence **8**, 1330–1335 (2015)
16. Y.S.M. Alajerami, S. Hashim, S.K. Ghoshal, M.A. Saleh, T. Kadni, M.I. Saripan, K. Alzimami, Z. Ibrahim, D.A.Bradley, The Effectof TiO_2 and MgO on the Thermoluminescence Properties of a Lithium Potassium Borate Glass System. J.Phys. Chem. Solids **74**, 1816–1822 (2013)
17. M.A. Marzouk, E.M. Abou, Hussein, Induced defects by gamma irradiation doses on the structure and optical behavior of undoped and TiO_2, Cr_2O_3, or MnO-doped heavy metal borate glasses. J. Appl. Phys. **125**, 1–11 (2019)
18. E.M. Abou Hussein, A.M. Madbouly, N.A. El, Alaily, Gamma ray interaction of optical, chemical, physical behavior of bismuth silicate glasses and their radiation shielding proficiency using Phy-X / PSD program. J. Non-Cryst. Solids **570**, 121021 (2021)
19. L. Nattapol, P. Panida, K. Pinit, K. Phetlada, T. Weerinradah, P.Ratchadaporn, J. Non-Cryst. Solids **453**, 118–122 (2016)
20. E.M. Abou, Hussein, Vitrified municipal waste for the immobilization of radioactive waste: preparation and characterization of borosilicate glasses modified with metal oxides. Silicon **11**(6), 2675–2688 (2019)
21. M.I.A. Abdel Maksoud 1, E.M. Abou Hussein, S.M. Kassem, R.A. Fahim, A.S. Awed, Effect of CeO_2 addition on structural, optical, and radiation shielding properties of $B_2O_3–Na_2O–SrO$ glass system. J. Mater. Sci.: Mater. Electron. **32**, 18931–18950 (2021)
22. E.M. Abou Hussein, N. A. El–Alaily, Study on the Effect of Gamma Radiation on Some Spectroscopic and Electrical Properties of Lithium Borate Glasses. J. Inorg. Organomet. Polym Mater. **28**, 1214–1225 (2018)
23. S. Manjeet, M.S. Dahiy, S. Dahiya, Khasa, Satish Khasa, Structural, optical and thermal properties of transition metal ions doped bismuth borate glasses. Eur. J. Glass Sci. Tech. B Phys. Chem. Glasses **57**, 45–52 (2016)
24. E.M. Abou Hussein, A.M. Madbouly, F.M. Ezz Eldin, N.A. ElAlaily, Evaluation of physical and radiation shielding properties of $Bi_2O_3–B_2O_3$ glass doped transition metals ions. Mater. Chem. Phys. **261**, 124212 (2021)
25. E.M. Abou Hussein, A.M. Madbouly, F.M. Ezz, Eldin, Characterization of some radiation shielding, optical, and physical properties of fluorophosphates glasses modified by Sm^{3+}. J. Mater. Sci.: Mater. Electron. (2021). https://doi.org/10.1007/s10854-021-05368-w

26. S. Baccaro, G. Monika, K.S. Sharma, Thind, D.P. Singh, Variation of optical band gap with radiation dose in $PbO–B_2O_3$ glasses. J. Nucl. Instrum. Methods Phys. Res., Sect. B. **266**, 594–598 (2008)
27. B. Ashok, V. Kumar, R. Kistaiah, Effect of alkaline earths on spectroscopic and structural properties of Cu^{2+} ions-doped lithium borate glasses. J. Non-Cryst. Solids **426**, 47–54 (2015)
28. E. M. Abou Hussein, Characterization of Some Chemical and Physical Properties of Lithium Borate Glasses Doped With CuO and/or TeO2 J.Chem. Soc. Pak., 41 (2019)-8
29. H.A. El Batal, E.M. Abou Hussein, N.A. El Alaily, F.M. EzzEldin, Effect of different 3d transition metal oxides on some physical properties of γ-Irradiated Bi_2O_3-B_2O_3 glasses: a comparative study. J. Non-Cryst. Solids **528**, 119–133 (2020)
30. D. Moncke, D. Ehrt, *Materials Science, Photoionization of polyvalent ions, Research Horizons* (Nova Science Publishers Inc, New York, 2007), p. 1
31. J.A. Duffy, Phys. Chem. Glasses **38**, 289–292 (1997)
32. F.H. El Batal, A.A. El Kheshen, M.A. Azooz, S.M. Abo-Naf, Gamma-ray interaction with lithium diborate glasses containing transition metals ions. J. Opt. Mater. **30**, 881–891 (2008)
33. I. Kashif, A. Ratep, Role of copper metal or oxide on physical properties of lithium borate glass. J. Mol. Struct. **1102**, 1–5 (2015)
34. N.F. Mott, E.A. Davis, *Electronic Processes in Non-crystalline Materials*, 2nd edn. (Clarendon Press, Oxford, UK, 1979)
35. C. Feifei, D. Shixun, N. Qiuhua, X. Tiefeng, S. Xiang, W. Xunsi, Glass Formation and Optical Band Gap Studies on Bi_2O_3 – B_2O_3 – BaO Ternary System System, Wuhan Univ. Technol. Mater. Sci. Ed. **24**, 716–720 (2009)
36. S.M. Abo-Naf, R.L. Elwan, M.A. Marzouk, Structure–property correlations in the SiO_2–PbO–Bi_2O_3 glasses. Mater. Sci. Mater. Electron. **23**, 1022–1030 (2012)
37. I. Kashif, S.A. Rahman, A.A. Soliman, E.M. Ibrahim, E.K. Abdel- Khalek, A.G. Mostafa, A.M. Sanad, Effect of alkali content on AC conductivity of borate glasses containing two transition metals. Phys. B **404**, 3842–3849 (2009)
38. S.W. Ghann, H. Kang, T. Sheikh, S. Yadav, T. Chavez-Gil, F. Nesbitt, J. Uddin, Fabrication, optimization and characterization of natural dye sensitized solar cell". Journal of Science Replication **7**(1), 1–12 (2017)

Figures

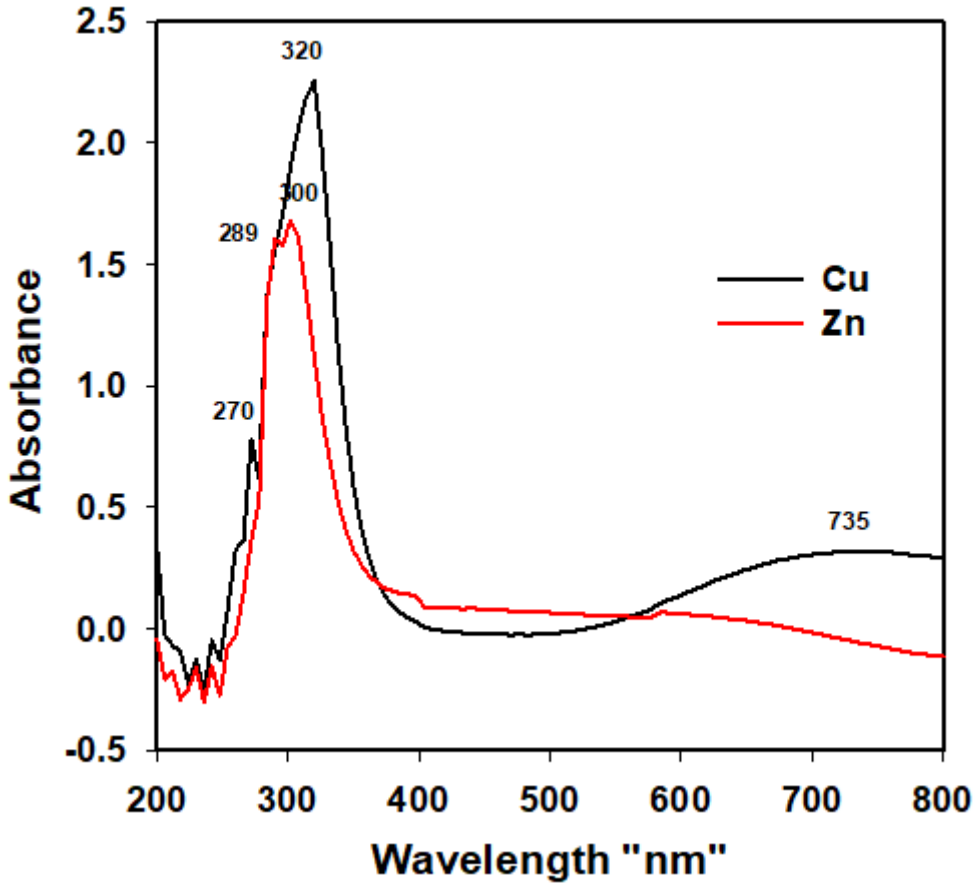

Figure 1

Optical absorbance of Cu and Zn doped borate glass systems

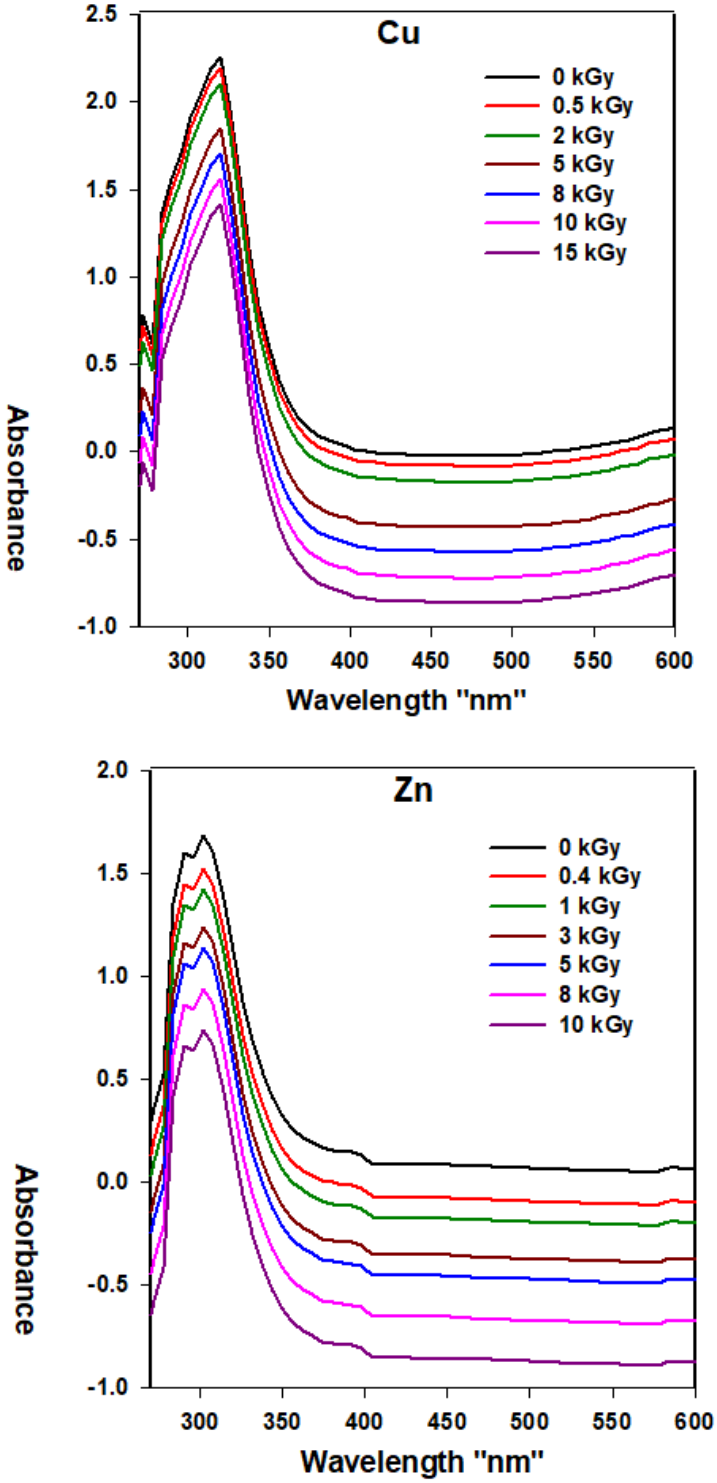

Figure 2

a& b. Absorption spectra of un-irradiated and irradiated Cu and Zn glasses

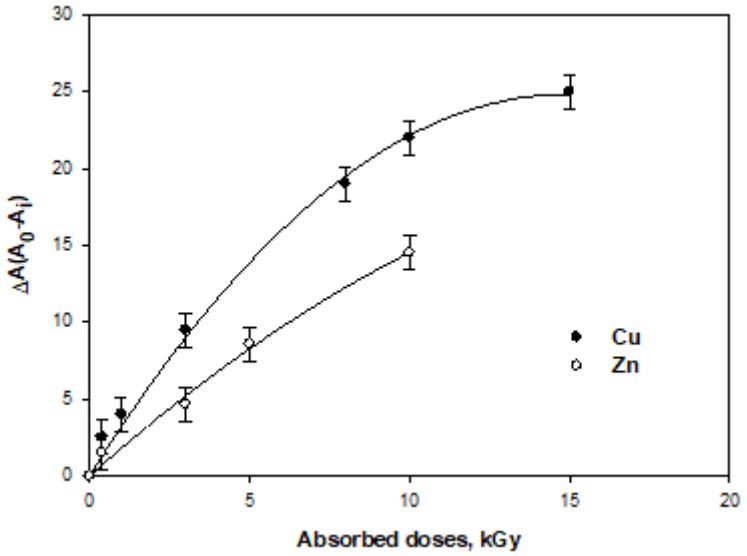

Figure 3

Change of ΔA, as a function of absorbed dose for different Cu and Zn doped glass borate samples.

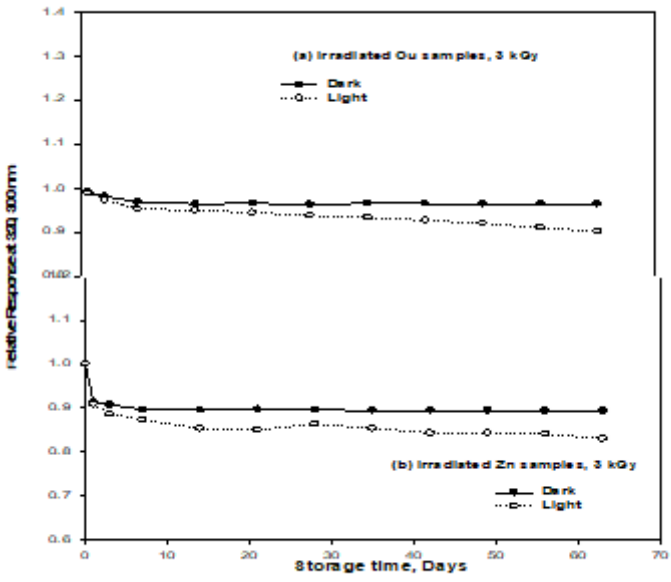

Figure 4

Color stability after irradiation (a- Cu glass samples) and irradiated (b- Zn glass samples) stored in the dark and under laboratory light.

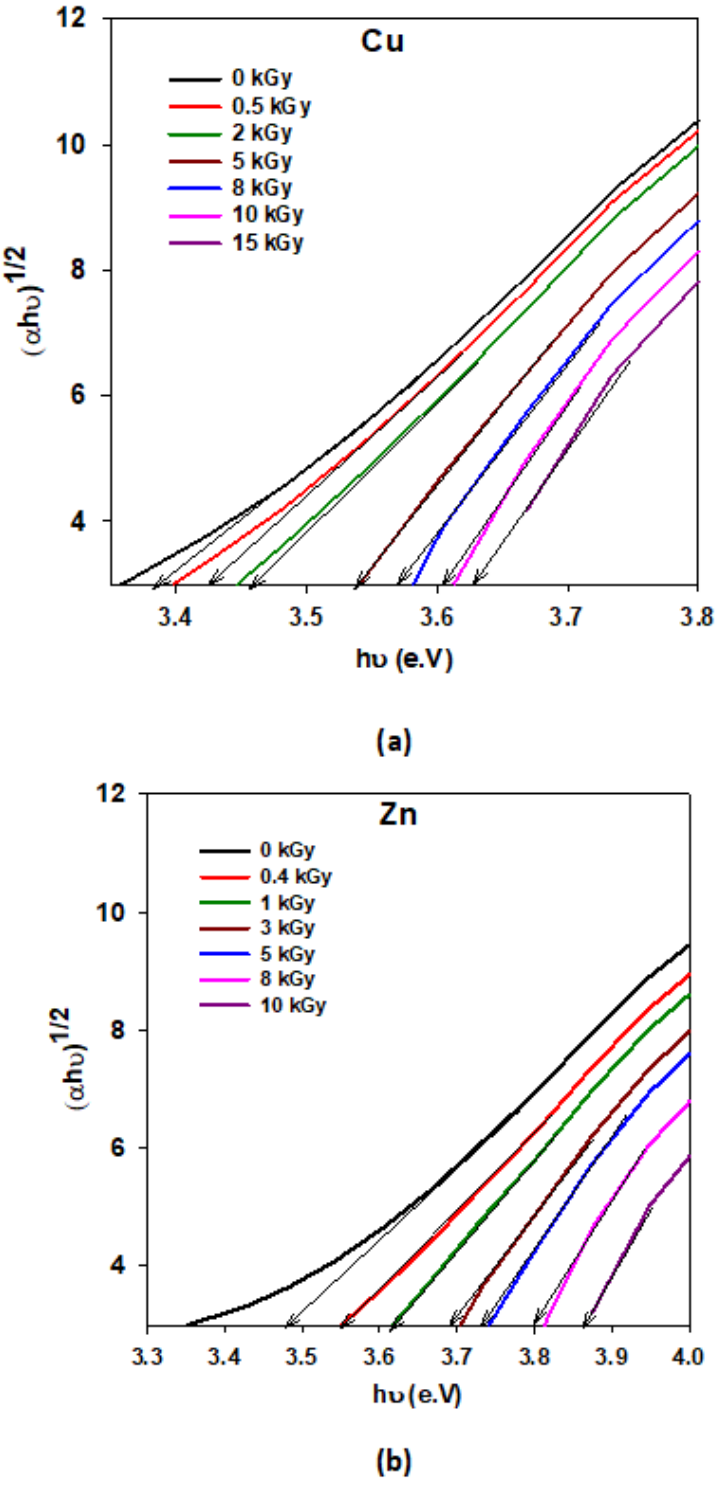

Figure 5

(a,b) Plots of (αhυ) 1/2 against hυ for Cu and Zn borate glasses before and after gamma irradiation doses.

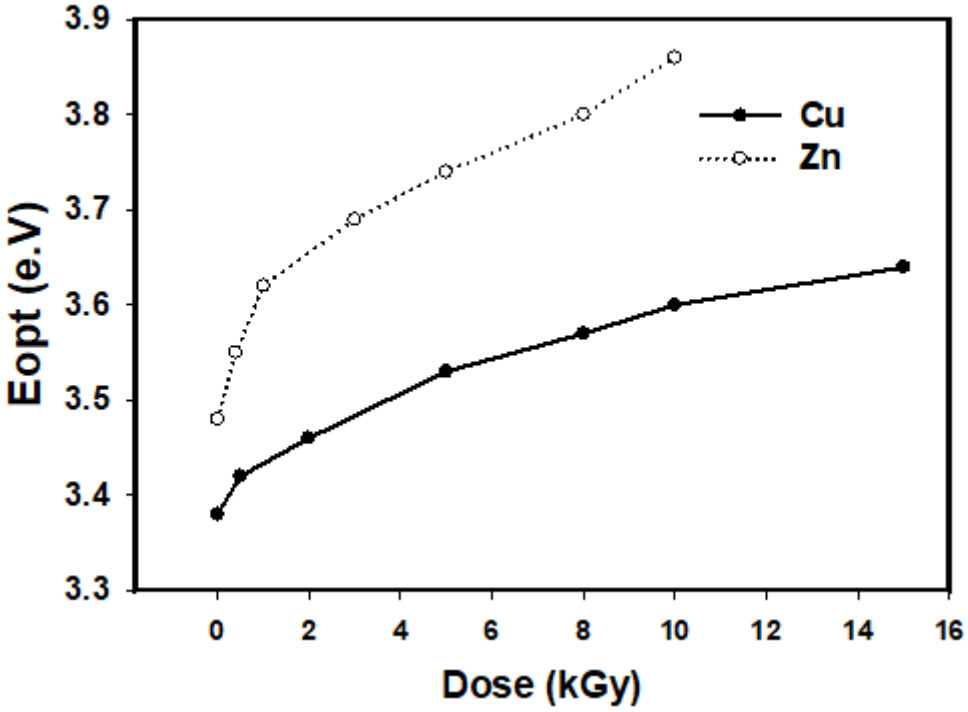

Figure 6

Response curve of Eopt values against dose of gamma radiation

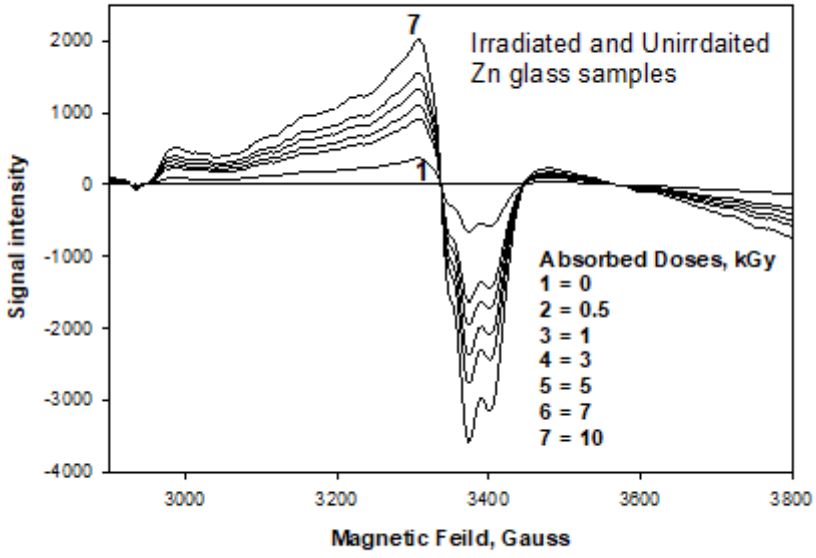

Figure 7

EPR spectra of un-irradiated and irradiated Zn-glass to different absorbed doses.

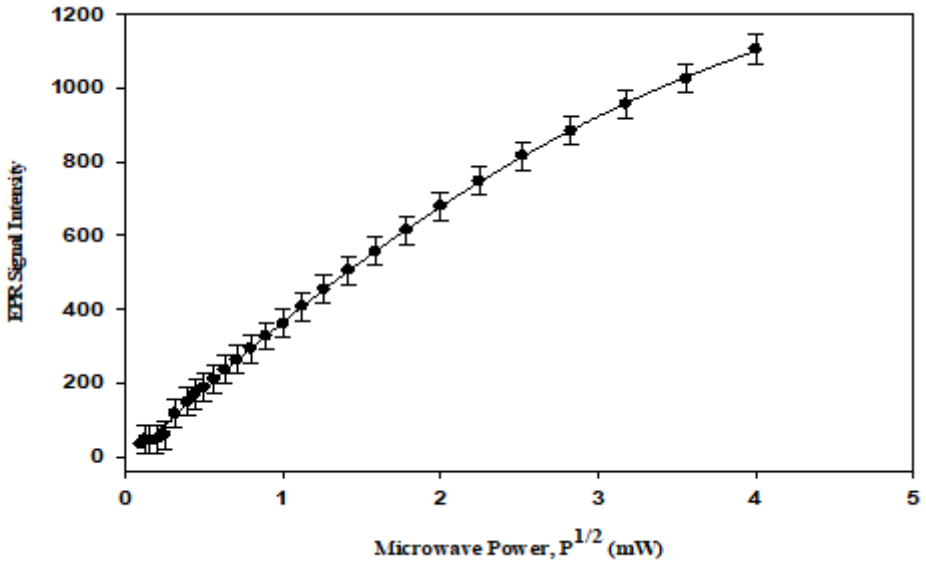

Figure 8

The dependence of EPR signal intensity (g-factor 2.01075) on microwave power, (for Zn –glass samples).

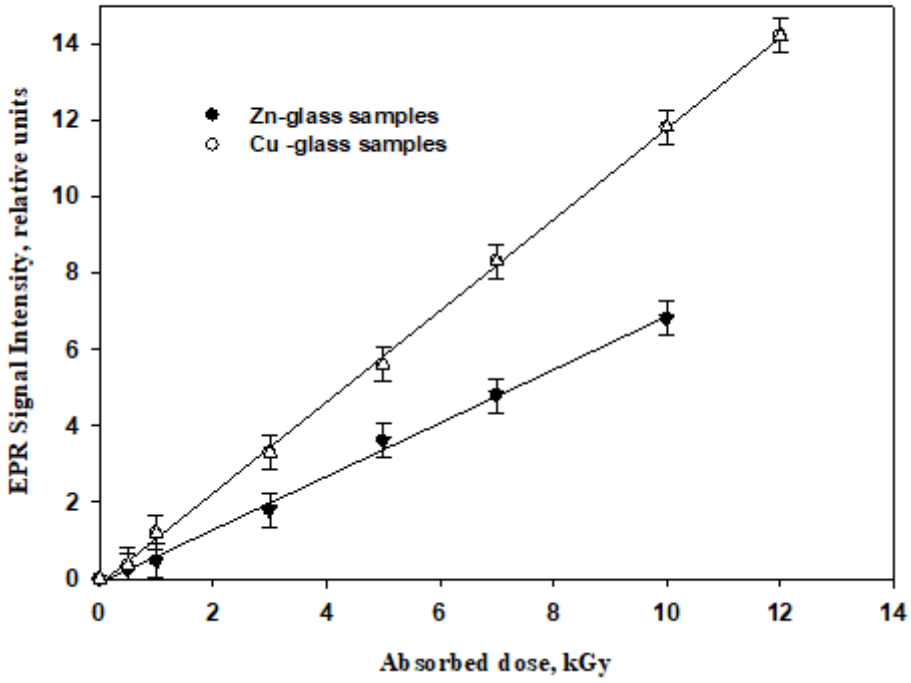

Figure 9

Dose-Response curves of Zn /Cu glass samples pellets dosimeter irradiated by 60Co γ-rays.

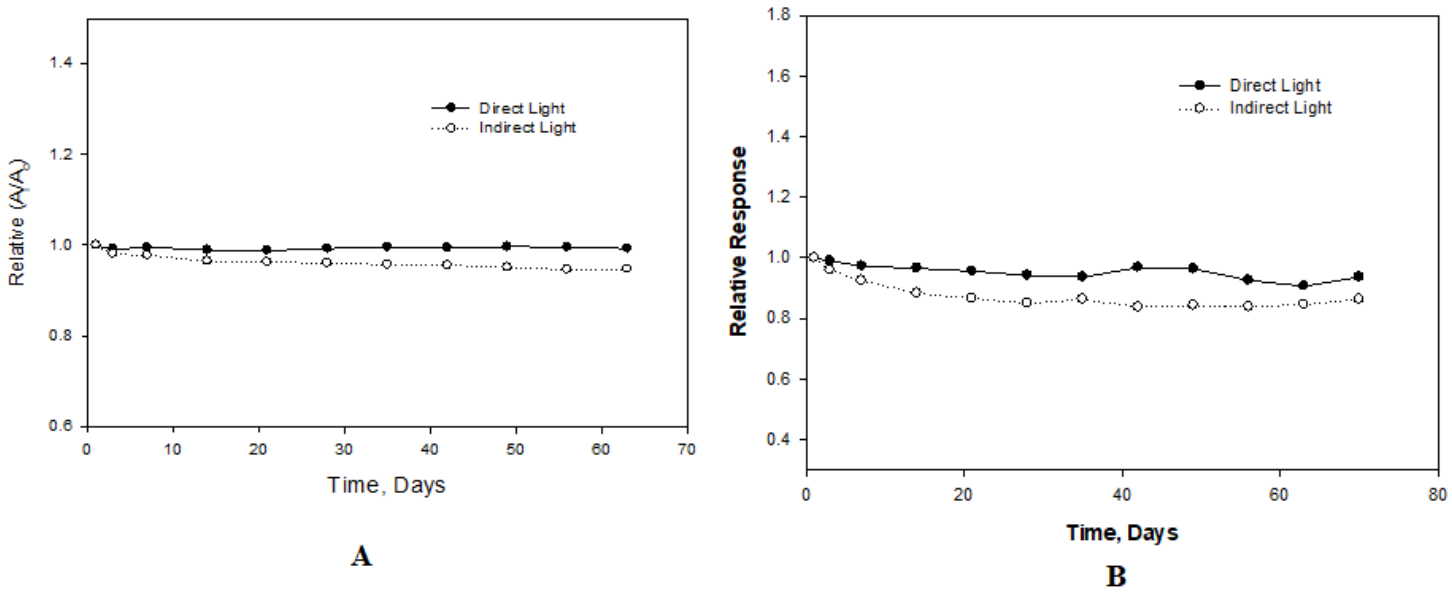

Figure 10

a. Pre-irradiation stability of Cu doped borate glass. b. Pre-irradiation stability of Zn doped borate glass.

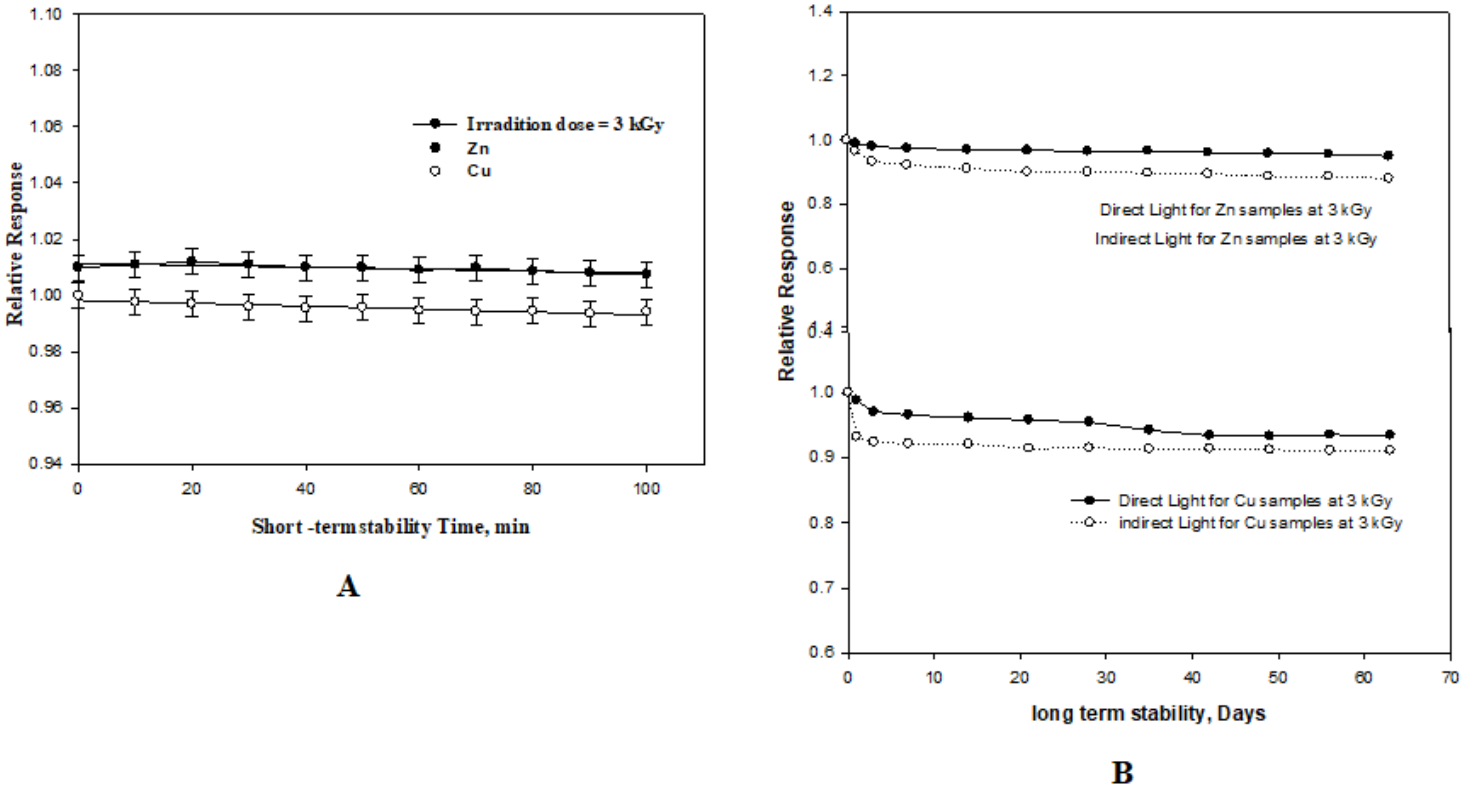

Figure 11

(a) EPR short-term stability after irradiation of Zn/Cu glass samples at 3 kGy (100 min. Immediately after irradiation) (b) EPR- long-term stability after irradiation of Cu/Zn glass samples at 3 kGy.

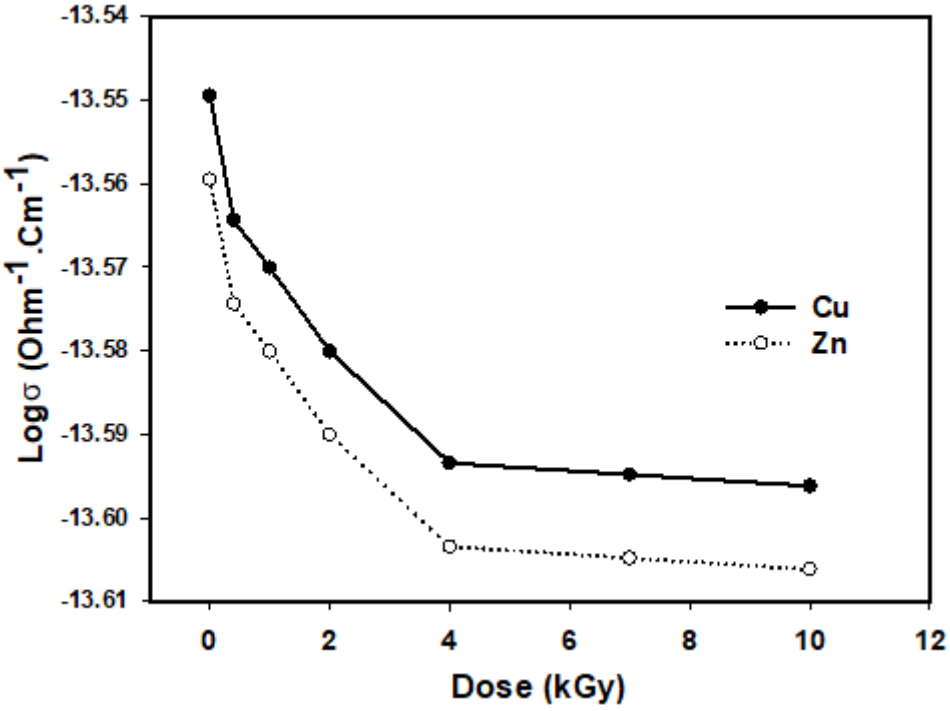

Figure 12

DC electrical conductivity of Cu and Zn glasses against radiation doses

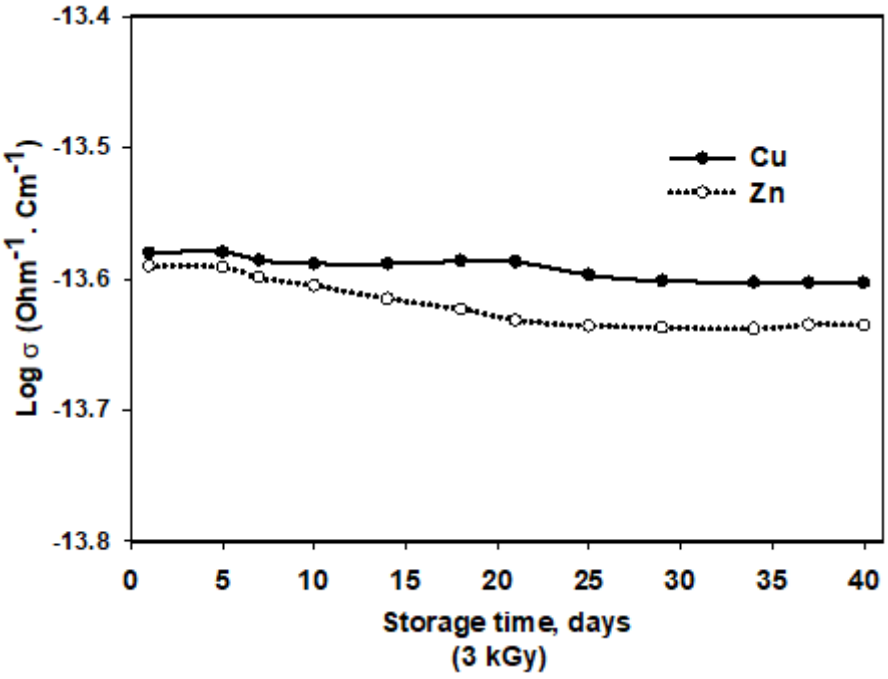

Figure 13

Long electric stability of irradiated Cu and Zn glasses (3 kGy)